

A Cascaded Two-Step Kalman Filter for Estimation of Human Body Segment Orientation Using MEMS-IMU

S. Zihajehzadeh, D. Loh, M. Lee, R. Hoskinson, and E.J. Park, *Senior Member, IEEE*

Abstract— Orientation of human body segments is an important quantity in many biomechanical analyses. To get robust and drift-free 3-D orientation, raw data from miniature body worn MEMS-based inertial measurement units (IMU) should be blended in a Kalman filter. Aiming at less computational cost, this work presents a novel cascaded two-step Kalman filter orientation estimation algorithm. Tilt angles are estimated in the first step of the proposed cascaded Kalman filter. The estimated tilt angles are passed to the second step of the filter for yaw angle calculation. The orientation results are benchmarked against the ones from a highly accurate tactical grade IMU. Experimental results reveal that the proposed algorithm provides robust orientation estimation in both kinematically and magnetically disturbed conditions.

I. INTRODUCTION

In many ambulatory biomechanical analyses, motion tracking of human body segments by accurate determination of each segment's orientation is of key importance [1]-[2]. The diverse application of body segment motion tracking ranges from rehabilitation and physical medicine to sports science [3]-[4]. Recently, with the advances in MEMS technology, miniature inertial measurement units (IMU) have emerged for wearable motion capture technology. These wearable miniature IMU, which consist of accelerometers, gyroscopes and magnetometers, together with a sensor fusion algorithm, can be used to estimate accurate orientation of human body segments to monitor a person's physical activities in daily life environment over an extended time period [5]-[6]. A 3-D orientation estimate can be obtained by integrating the angular velocities from the tri-axial gyroscope, but, this causes unbounded orientation drift due to the gyroscope's output noise. In order to compensate for this error, accelerometer and magnetometer are employed as the vertical (the gravity) and horizontal (the Earth's magnetic field) references, respectively [5].

To estimate the full 3-D orientation (roll, pitch, and yaw), most researchers have focused on fusing data from the above sensor triplets in a Kalman filter together with an optimization algorithm. The widely used optimization algorithms for this purpose, such as QUEST [4], O2OQ [5]

and G-N [1], provide the optimal orientation from accelerometer and magnetometer output vector for measurement update step in the Kalman filter. To use these optimization methods, it should be assumed that constant reference vector measurements (i.e. the gravity from the accelerometer and Earth magnetic field from the magnetometer) are available, which cannot be guaranteed [5]. To deal with this problem, most authors use a threshold-based switching approach [7] or a vector selector algorithm [5] to ignore the perturbed acceleration and/or magnetic field measurement in the Kalman filter. In spite of their accuracy, these optimization algorithms have high computational costs. On the other hand, without employing such optimization, another method to estimate orientation in kinematically and/or magnetically disturbed conditions is to include acceleration model and magnetic field model in the orientation estimation Kalman filter. One complementary Kalman filter approach is presented in [8] for 2-D orientation estimation and is extended to 3-D orientation in [9].

This paper introduces a novel fast two-step cascaded Kalman filter for orientation estimation without using optimization. The proposed algorithm uses two linear Kalman filters, consisting of a tilt angle (roll and pitch) Kalman filter followed by a yaw (heading) angle Kalman filter. The first step is based on our previous algorithm in [10], which uses the accelerometers' output vector along with an acceleration model to accurately estimate the tilt angles. The second step extends our tilt angle algorithm to full 3-D orientation by a novel yaw angle estimation method. Using this proposed method, the effect of ferromagnetic disturbances is completely decoupled from the tilt angle estimation. Furthermore, the estimated tilt angles in the first step help to determine the yaw angle in the second step more accurately.

II. METHOD

A. Problem Definition

The orientation of the sensor frame (the frame fixed to sensor) with respect to an inertial frame (the frame pointing to local East, North and Up directions) can be represented by a rotation matrix which maps a vector from the sensor frame to the inertial frame:

$${}^I\mathbf{x} = {}^I\mathbf{R} {}^S\mathbf{x} \quad (1)$$

where \mathbf{x} is an arbitrary 3×1 vector and left superscripts I and S represent the inertial and sensor frame respectively. ${}^I\mathbf{R}$ is the 3×3 rotation matrix expressed as [10]:

$${}^I\mathbf{R} = \begin{bmatrix} \text{cac}\beta & \text{cas}\beta\text{sy} - \text{sac}\gamma & \text{cas}\beta\text{c}\gamma + \text{sas}\gamma \\ \text{sac}\beta & \text{sas}\beta\text{sy} + \text{cac}\gamma & \text{sas}\beta\text{c}\gamma - \text{cas}\gamma \\ -\text{s}\beta & \text{c}\beta\text{sy} & \text{c}\beta\text{c}\gamma \end{bmatrix} \quad (2)$$

This work is supported by the Natural Sciences and Engineering Research Council of Canada (NSERC) and the experimental protocol (No, 2013s0790) is approved by the Office of Research Ethics of Simon Fraser University.

S. Zihajehzadeh, D. Loh, M. Lee and E.J. Park are with the School of Mechatronic Systems Engineering, Simon Fraser University, 250-13450 102nd Avenue, Surrey, BC, Canada, V3T 0A3 (email: szihajeh@sfu.ca, dj18@sfu.ca, tla18@sfu.ca, ed_park@sfu.ca)

R. Hoskinson is with Recon Instruments Inc., 1050 Homer Street, Vancouver, BC, Canada, V6B 2W9 (email: reynald@reconinstruments.com)

where c and s are abbreviations for \cos and \sin respectively; α (yaw), β (pitch) and γ (roll) are the rotation angles about the Z -, Y -, and X - axes of the inertial frame respectively. Note that the last row of the rotation matrix is the unit gravity vector expressed in the sensor frame and is independent from yaw angle [10]. By estimating this row, roll and pitch (tilt) angles can be determined:

$$\gamma = \tan^{-1}\left(\frac{{}^s\mathbf{R}_{3,2}}{{}^s\mathbf{R}_{3,3}}\right), \beta = \tan^{-1}\left(\frac{-{}^s\mathbf{R}_{3,1}}{{}^s\mathbf{R}_{3,2}/\sin\gamma}\right) \quad (3)$$

where ${}^s\mathbf{R}_{i,j}$ represents the i^{th} row and j^{th} column in rotation matrix ${}^s\mathbf{R}$. Additionally, by estimating the first row in rotation matrix and having the tilt angles, yaw angle (α) can be readily determined by:

$$\alpha = \tan^{-1}\left(\frac{-c\gamma {}^s\mathbf{R}_{1,2} + s\gamma {}^s\mathbf{R}_{1,3}}{{}^s\mathbf{R}_{1,1}/c\beta}\right) \quad (4)$$

In this work, a two-step cascaded Kalman filter is used to determine full 3-D orientation including tilt angles and yaw angle. In the first step, i.e. the tilt Kalman filter, gyroscope and accelerometer data are used along with an acceleration model, to estimate the last row of the orientation matrix in order to calculate the tilt angles. In the second step, gyroscope and magnetometer data are used along with the estimated tilt angles from the first step to accurately estimate the first row of the rotation matrix to determine the yaw angle.

The structure of the tilt Kalman filter and the yaw Kalman filter is explained in the following sections.

A. Tilt Kalman Filter

The tilt Kalman filter is based on the algorithm presented in our previous work [10], which allows accurate determination of the roll and pitch angles under dynamic conditions. In this method, the measurements from the tri-axial gyroscopes and tri-axial accelerometers are used in a Kalman filter to estimate the normalized gravity vector in the sensor frame (i.e., the third row of the rotation matrix ${}^s\mathbf{R}$) using the following system model equations [10]:

$$\mathbf{x}_1(k) = \mathbf{A}_1(k-1) \mathbf{x}_1(k-1) + \mathbf{w}_1(k-1) \quad (5)$$

$$\mathbf{z}_1(k) = \mathbf{C}_1(k) \mathbf{x}_1(k) + \mathbf{v}_1(k) \quad (6)$$

In Eqs. (5) and (6), $\mathbf{x}_1(k) = [-s\beta \ c\beta s\gamma \ c\beta c\gamma]^T$ is the 3×1 state vector for tilt angles Kalman filter at step k ; \mathbf{A}_1 is the state transition matrix and \mathbf{w}_1 is the process model noise vector; \mathbf{z}_1 is the measurement vector (i.e. the normalized measured gravity vector in the sensor frame); \mathbf{C}_1 is the 3×3 observation matrix; and \mathbf{v}_1 is the measurement model noise vector. The matrices in (5) and (6) can be calculated using the following equations [10]:

$$\mathbf{A}_1(k-1) = \mathbf{I} - \Delta t \tilde{\mathbf{y}}_G(k-1) \quad (7)$$

$$\mathbf{w}_1(k-1) = \Delta t(-\tilde{\mathbf{x}}_1(k))\mathbf{n}_G \quad (8)$$

$$\mathbf{C}_1(k) = \mathbf{g} \mathbf{I}_3 \quad (9)$$

$$\mathbf{v}_1(k) = -{}^s\mathbf{a}_\varepsilon^-(k) + \mathbf{n}_A \quad (10)$$

$${}^s\mathbf{a}_\varepsilon^-(k) = {}^s\mathbf{a}^-(k) - {}^s\mathbf{a}(k) \quad (11)$$

$${}^s\mathbf{a}^-(k) = c_a {}^s\mathbf{a}^+(k-1) \quad (12)$$

where $\tilde{\mathbf{y}}_G$ is the 3×3 skew symmetric matrix of tri-axial gyroscope measurements; $\tilde{\mathbf{x}}_1$ is the 3×3 skew symmetric

matrix of \mathbf{x}_1 ; ${}^s\mathbf{a}_\varepsilon^-(k)$ is the external acceleration error in the sensor frame; \mathbf{n}_G and \mathbf{n}_A are the gyroscope and accelerometer measurement noise vectors, which are assumed to be uncorrelated and zero-mean white Gaussian; the superscripts $+$ and $-$ stand for the “*a posteriori*” and the “*a priori*” estimates in the Kalman filter, respectively; c_a is a dimensionless constant between 0 and 1 that determines the cut-off frequency in the external acceleration model (${}^s\mathbf{a}(k) = c_a {}^s\mathbf{a}(k-1) + \boldsymbol{\varepsilon}(k)$, with $\boldsymbol{\varepsilon}(k)$ being the time-varying error of the external acceleration process model); ${}^s\mathbf{a}^+(k-1)$ is the gravity compensated external acceleration; and \mathbf{g} is the norm of gravity vector.

The measurement vector in Eq. (6) is calculated by [10]:

$$\mathbf{z}_1(k) = \mathbf{y}_A(k) - c_a {}^s\mathbf{a}^+(k-1) \quad (13)$$

$${}^s\mathbf{a}^+(k) = \mathbf{y}_A(k) - \mathbf{g} \mathbf{x}_1^+(k) \quad (14)$$

where $\mathbf{y}_A(k)$ is the bias compensated output vector of the accelerometer.

The process and measurement noise covariance matrices in the tilt Kalman filter, $\mathbf{Q}_1(k-1)$ and $\mathbf{R}_1(k)$, are calculated using the following equations:

$$\begin{aligned} \mathbf{Q}_1(k-1) &= E[\mathbf{w}_1(k-1) \mathbf{w}_1(k-1)^T] \\ &= -\Delta t^2 \tilde{\mathbf{x}}_1(k-1) \boldsymbol{\Sigma}_G \tilde{\mathbf{x}}_1(k-1) \end{aligned} \quad (15)$$

$$\mathbf{R}_1(k) = E[\mathbf{v}_1(k) \mathbf{v}_1(k)^T] = \boldsymbol{\Sigma}_{\text{acc}} + \boldsymbol{\Sigma}_A \quad (16)$$

where $\boldsymbol{\Sigma}_G$ is the covariance matrix of the gyroscope’s measurement noise which is defined as $E[\mathbf{n}_G \mathbf{n}_G^T]$. By assuming that the gyro noise variances are equal to σ_G^2 in the three axes, $\boldsymbol{\Sigma}_G$ is set to $\sigma_G^2 \mathbf{I}_3$. Similar to $\boldsymbol{\Sigma}_G$, $\boldsymbol{\Sigma}_A$ which is the covariance matrix of accelerometer’s measurement noise, is set to $\sigma_A^2 \mathbf{I}_3$. $\boldsymbol{\Sigma}_{\text{acc}}$ is the covariance of the acceleration model and is set to $3^{-1} c_a^2 \|{}^s\mathbf{a}^+(k-1)\|^2$.

Using the estimated normalized gravity vector in the sensor frame, $\mathbf{x}_1^+(k) = [x_{1,x} \ x_{1,y} \ x_{1,z}]^T$, the desired roll (γ) and pitch (β) angles are calculated using (3):

$$\gamma(k) = \tan^{-1}\left(\frac{x_{1,y}}{x_{1,z}}\right), \beta(k) = \tan^{-1}\left(\frac{-x_{1,x}}{x_{1,y}/\sin\gamma}\right) \quad (17)$$

As illustrated in Fig. 1, these two tilt angles are the inputs to the second step, i.e. the yaw Kalman filter.

B. Yaw Kalman Filter

The yaw angle Kalman filter allows accurate determination of yaw angle under temporary ferromagnetic disturbances. In this Kalman filter, the measurements from tri-axial gyroscopes and tri-axial magnetometers and the known tilt angles are used to estimate the first row of the rotation matrix ${}^s\mathbf{R}$. The system model equations are represented by:

$$\mathbf{x}_2(k) = \mathbf{A}_2(k-1) \mathbf{x}_2(k-1) + \mathbf{w}_2(k-1) \quad (18)$$

$$\mathbf{z}_2(k) = \mathbf{C}_2(k) \mathbf{x}_2(k) + \mathbf{v}_2(k) \quad (19)$$

where $\mathbf{x}_2(k) = [cac\beta \ cas\beta s\gamma - sac\gamma \ cas\beta c\gamma + sas\gamma]^T$ is the 3×1 state vector for heading angle Kalman filter at step k and \mathbf{A}_2 , \mathbf{w}_2 and \mathbf{C}_2 can be calculated as:

$$\mathbf{A}_2(k-1) = \mathbf{I} - \Delta t \tilde{\mathbf{y}}_G(k-1) \quad (20)$$

$$\mathbf{w}_2(k-1) = \Delta t(-\tilde{\mathbf{x}}_2(k))\mathbf{n}_G \quad (21)$$

$$\mathbf{C}_2(k) = \mathbf{I}_3 \quad (22)$$

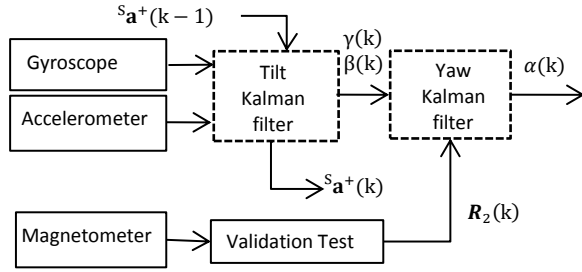


Fig. 1. Overview of the proposed algorithm structure

To calculate the measurement vector $\mathbf{z}_2(k)$, roll, pitch and yaw angles at each step k are required. However, at each step, roll and pitch are already known from the tilt Kalman filter. Since these tilt angles are used in calculation of $\mathbf{z}_2(k)$ for the measurement update of yaw Kalman filter, they are called ‘measured tilt angles’ and denoted by β_m and γ_m . To get the ‘measured yaw angle’, α_m , for complete calculation of $\mathbf{z}_2(k)$, magnetometer data is used in the following algorithm:

1) The rotation matrix with respect to local horizontal plane, ${}^S\mathbf{R}_{\gamma_m, \beta_m}$, is calculated using the known tilt angles:

$${}^S\mathbf{R}_{\gamma_m, \beta_m} = \begin{bmatrix} \cos \beta_m & 0 & \sin \beta_m \\ 0 & 1 & 0 \\ -\sin \beta_m & 0 & \cos \beta_m \end{bmatrix} \begin{bmatrix} 1 & 0 & 0 \\ 0 & \cos \gamma_m & -\sin \gamma_m \\ 0 & \sin \gamma_m & \cos \gamma_m \end{bmatrix} \quad (23)$$

2) The output vector of the magnetometer, \mathbf{y}_M , is rotated using the horizontal rotation matrix ${}^S\mathbf{R}_{\gamma_m, \beta_m}$. The rotated vector is expressed by ${}^{tilt}\mathbf{y}_M$. The horizontal component of the rotated vector is located in the horizontal plane (East-North plane) of the navigation frame.

$${}^{tilt}\mathbf{y}_M = {}^S\mathbf{R}_{\gamma_m, \beta_m} \mathbf{y}_M \quad (24)$$

3) The measured yaw angle, α_m , is calculated as the angle between the horizontal component of ${}^{tilt}\mathbf{y}_M$ and that of the Earth’s magnetic field.

Then, $\mathbf{z}_2(k)$ can be calculated as:

$$\mathbf{z}_2(k) = [c\alpha_m c\beta_m \quad c\alpha_m s\beta_m s\gamma_m - s\alpha_m c\gamma_m \quad c\alpha_m s\beta_m c\gamma s\alpha_m s\gamma_m]^T \quad (25)$$

However, under temporary magnetic disturbances, the magnetometer output vector cannot be trusted as reliable information. To avoid the effect of disturbed magnetic field on the estimated yaw angle, a threshold-based switching approach similar to the method in [8] is employed. In the threshold-based switching method, the measured magnetic field is tested for significant deviations from the local earth’s magnetic field. This validation test excludes the disturbed measurement by assigning a large measurement noise value in the yaw Kalman filter. As a result, $\mathbf{R}_2(k)$, the measurement noise covariance matrix for the yaw Kalman filter is defined as:

$$\mathbf{R}_2(k) = \begin{cases} \sigma_M^2 \mathbf{I}_3 & \|\mathbf{y}_M(k) - \mathbf{h}\| < \varepsilon_M \cap |\theta_{dip} - \theta_{dip, t=0}| < \varepsilon_{dip} \\ \infty & \text{Otherwise} \end{cases} \quad (26)$$

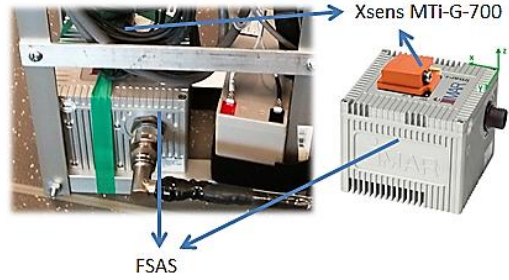


Fig. 2. Experimental setup: Xsens MTi-G-700 attached to reference IMU-FSAS

where σ_M^2 is the magnetometer noise variance in each axis. θ_{dip} is the current dip angle (i.e. the angle formed by the gravity vector and current magnetic field vector) and θ_{dip} is its initial value. ε_M and ε_{dip} are the threshold values.

Finally, $\mathbf{Q}_2(k)$ is defined similar to $\mathbf{Q}_1(k)$:

$$\mathbf{Q}_2(k-1) = -\Delta t^2 \tilde{\mathbf{x}}_2(k-1) \Sigma_G \tilde{\mathbf{x}}_2(k-1) \quad (27)$$

Using the best estimate of $\mathbf{x}_2(k)$ from yaw Kalman filter, $\mathbf{x}_2^+(k) = [x_{2,x} \quad x_{2,y} \quad x_{2,z}]^T$, the best estimate for yaw angle (α) can be calculated as:

$$\alpha(k) = \tan^{-1} \left(\frac{-c\gamma x_{2,y} + s\gamma x_{2,z}}{x_{2,x}/c\beta} \right) \quad (28)$$

The structure of the proposed two-step algorithm is shown in Fig. 1.

III. EXPERIMENTAL SETUP

In order to evaluate the performance of the proposed algorithm, raw inertial and magnetic data from Xsens MTi-G-700 at the rate of 100 Hz are used. The reference system uses IMU-FSAS (tactical grade IMU with fiber optic gyroscopes and servo accelerometers) integrated in Novatel SPAN system with inertial explorer post processing software. Orientation accuracy of the reference system is 0.008 deg for the roll and pitch angles and 0.023 deg for the yaw angle. The MTi-G-700 is attached on top of the IMU-FSAS using double-sided adhesive tape and the whole system is fixed to an aluminum frame (Fig. 2). This frame goes into a backpack that is worn by subjects. The gyro noise variance σ_G^2 and the accelerometer noise variance σ_A^2 are obtained from static measurements and are set to $10^{-4} \text{ Rad}^2/\text{s}^2$ and $10^{-4} \text{ m}^2/\text{s}^4$, respectively. ε_M , ε_{dip} and c_a are set to 10^{-2} , 2° and 0.3, respectively.

To examine the robustness of the algorithm against temporary ferromagnetic disturbance and medium to large human body accelerations, three different tests were performed. To be consistent with the output data of the reference system yaw angle is converted to heading angle.

IV. EXPERIMENTAL RESULTS AND DISCUSSION

A. Experiment 1: Ferromagnetic disturbance

In this experiment, MTi-G-700 is left stationary for 120 s and the magnetic field is temporarily disturbed using an iron disk for 5 s, 10 s and 15 s intervals. The normalized magnitude of the magnetic field and the calculated heading angle with and without the threshold-based switching is shown in Fig. 3. As it can be seen in this figure, the proposed algorithm with threshold-based switching rejects

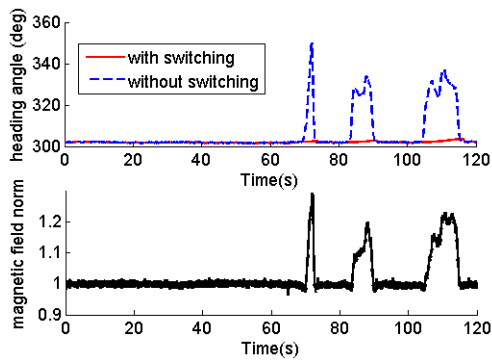


Fig. 3. Top: heading angle with and without threshold-based switching, Bottom: normalized magnetic field norm

the disturbances and the estimated heading angle remains stable during temporary ferromagnetic disturbances. A small heading drift can also be observed during the disturbance which is due to reliance of the algorithm on gyroscopes data.

B. Experiment 2: Large acceleration with short duration

To produce large acceleration, in this experiment, the subject is asked to wear the backpack and perform a vertical jump. Roll, pitch and heading angles along with the norm of the tri-axial accelerometer output vector during a typical vertical jump is shown in Fig. 4. As it can be seen in this figure, the acceleration norm is reached to a maximum of 40 m/s^2 . However, the algorithm can accurately track orientation even in the presence of the large acceleration.

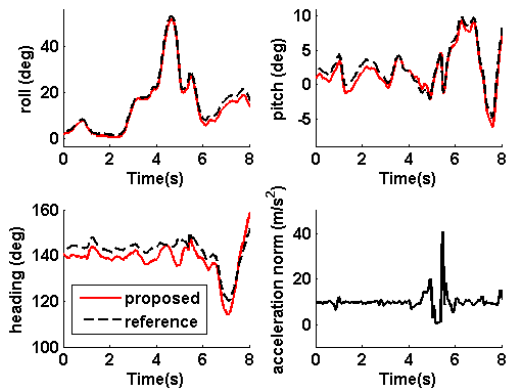


Fig. 4. Roll, pitch and heading angles during a typical vertical jump

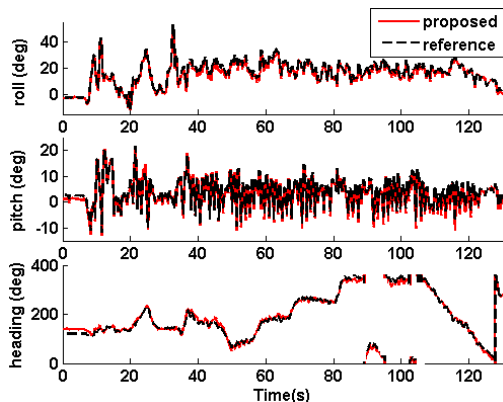


Fig. 5. Roll, pitch and heading angles during a rollerblading experiment (The discontinuities in the heading angle curve is due to its range being from 0 to 360 deg)

C. Experiment 3: Medium acceleration with long duration

To evaluate performance of the proposed algorithm for a typical motion with low to medium level of acceleration, the subject is asked to rollerblade outdoors while carrying the backpack. The orientation results presented in Fig. 5 show that the estimated orientation is reasonably good during the entire test duration and no orientation drift is observed.

V. CONCLUSION

This work proposes the use of a cascaded two-step Kalman filter for human body orientation determination using MEMS inertial/magnetic sensors. In the first step, accelerometers' data along with an acceleration model is used in a Kalman filter to accurately estimate tilt angles. In the second step, the estimated tilt angles along with magnetometers' data are used in a Kalman filter along accurately track the yaw angle. The yaw Kalman filter employs threshold-based switching method to deal with short-term magnetic disturbances. In comparison to the most popular orientation estimation algorithms, the proposed method does not use optimization for orientation estimation, which makes it computationally more efficient. Additionally, because of its two-step structure, the tilt angles would not be affected by a perturbed magnetic field while the estimated tilt angles help to determine yaw angle more accurately. Experimental results show that the proposed algorithm can cover various ranges of human body motions and is robust against temporary magnetic disturbances.

REFERENCES

- [1] J. K. Lee and E. J. Park, "A fast Gauss-Newton optimizer for estimating human body orientation.," *Conf. Proc. IEEE Eng. Med. Biol. Soc.*, Vancouver, British Columbia, Canada, Aug. 2008, pp. 1679–82.
- [2] H. P. Bruckner, C. Spindeldreier, and H. Blume, "Modification and fixed-point analysis of a Kalman filter for orientation estimation based on 9-D inertial measurement unit data.," *Conf. Proc. IEEE Eng. Med. Biol. Soc.*, Osaka, Japan, Jul. 2013, pp. 3953–6.
- [3] J. Favre, B. M. Jolles, R. Aissaoui, and K. Aminian, "Ambulatory measurement of 3D knee joint angle.," *J. Biomech.*, vol. 41, no. 5, pp. 1029–35, Jan. 2008.
- [4] X. Yun and E. R. Bachmann, "Design, Implementation, and Experimental Results of a Quaternion-Based Kalman Filter for Human Body Motion Tracking," *IEEE Trans. Robot.*, vol. 22, no. 6, pp. 1216–1227, Dec. 2006.
- [5] J.K. Lee and E.J. Park, "Minimum-Order Kalman Filter With Vector Selector for Accurate Estimation of Human Body Orientation," *IEEE Trans. Robot.*, vol. 25, no. 5, pp. 1196–1201, Oct. 2009.
- [6] Y. Teruyama and T. Watanabe, "A basic study on variable-gain Kalman filter based on angle error calculated from acceleration signals for lower limb angle measurement with inertial sensors.," *Conf. Proc. IEEE Eng. Med. Biol. Soc.*, Osaka, Japan, Jul. 2013, pp. 3423–6.
- [7] A. M. Sabatini, "Quaternion-based extended Kalman filter for determining orientation by inertial and magnetic sensing.," *IEEE Trans. Biomed. Eng.*, vol. 53, no. 7, pp. 1346–56, Jul. 2006.
- [8] H. J. Luinge and P. H. Veltink, "Measuring orientation of human body segments using miniature gyroscopes and accelerometers," *Med. Biol. Eng. Comput.*, vol. 43, no. 2, pp. 273–282, Mar. 2005.
- [9] D. Roetenberg, H. J. Luinge, C. T. M. Baten, and P. H. Veltink, "Compensation of magnetic disturbances improves inertial and magnetic sensing of human body segment orientation.," *IEEE Trans. Neural Syst. Rehabil. Eng.*, vol. 13, no. 3, pp. 395–405, Sep. 2005.
- [10] J. K. Lee, E. J. Park, and S. Robinovitch, "Estimation of attitude and external acceleration using inertial sensor measurement during various dynamic conditions," *IEEE Trans. Instrum. Meas.*, vol. 61, no. 8, pp. 2262–2273, Aug. 2012.